Intramolecular hydrogen bonding in hydroxylated semiquinones inhibits semiquinone–Mg^{2+} complex formation

Antonio E. Alegría,* Carmelo Garcia, Glyssette Santiago, Gladys Collazo and Julio Morant

University of Puerto Rico at Humacao, Department of Chemistry, CUH Station, Humacao, Puerto Rico 00791

Received (in Cambridge, UK) 18th January 2000, Accepted 14th April 2000
Published on the Web 2nd June 2000

Complex formation between the semiquinones of 5,8-dihydroxynaphtho-1,4-quinone, $NZQ^{\bullet -}$, 1,4-dihydroxyanthracene-9,10-dione, $QNZ^{\bullet -}$, benzo-1,4-quinone, $BQ^{\bullet -}$, and phenanthraquinone, $PHQ^{\bullet -}$, and Mg^{2+} was studied utilizing EPR spectroscopy. Weighted average EPR spectra between those corresponding to the uncomplexed and complexed semiquinones were observed for $NZQ^{\bullet -}$, $QNZ^{\bullet -}$ and $BQ^{\bullet -}$ while these species were observed simultaneously for $PHQ^{\bullet -}$. The semiquinones $NZQ^{\bullet -}$, $QNZ^{\bullet -}$ and $BQ^{\bullet -}$ behave as weak Mg^{2+} chelators while $PHQ^{\bullet -}$ chelates this cation much more strongly (binding constant = $(1.1 \pm 0.5) \times 10^3$ dm^3 mol^{-1}). The weak binding of Mg^{2+} by $NZQ^{\bullet -}$ and $QNZ^{\bullet -}$ is in contrast with the large complex formation constants between the parent quinones NZQ and QNZ and different metal cations. This apparent paradox is explained by the strong intramolecular hydrogen bonding existing in $NZQ^{\bullet -}$ and $QNZ^{\bullet -}$.

Introduction

Semiquinones are important intermediates in electron transfer reactions in natural and artificial systems, such as those involved in cell respiration,[1] photosynthesis[2] and cytotoxic processes[3]. Most semiquinones are anionic species in aqueous solutions at neutral pH (pK_a near 4),[4–6] thus the interaction of semiquinones with metal counterions should have an effect on the efficiencies of the semiquinone-mediated reactions indicated above.

Among the cytotoxic quinones, the anthracycline-type quinones, such as adriamycin and daunomycin, are well-known for their very large complex formation constants with transition metal ions ($>10^{11}$).[7,8] Redox-active metals bound to anthracycline quinones have been postulated to play a decisive role in anthracycline antitumor[9] and cardiotoxic activities.[10] However, very little is known regarding the ability of these semiquinones to chelate cations in aqueous solutions. To the best of our knowledge, one manuscript exists where an anthracycline semiquinone is reported to have a weak interaction with Fe^{3+}.[11] Electrochemical methods were used in that work to probe this interaction and a non-aqueous solvent, dimethylformamide, was used.

In this work we have followed the ion-pair formation process between semiquinones and Mg^{2+} using electron paramagnetic resonance (EPR) spectroscopy. Since the anthracycline semiquinones of daunomycin and adriamycin are not stable species in solution,[12,13] these are represented here by other quinones with anthracycline-type structure, *i.e.* with hydroxy groups at *peri* positions relative to the carbonyl groups. These are 5,8-dihydroxynaphtho-1,4-semiquinone, $NZQ^{\bullet -}$, and 1,4-dihydroxyanthracene-9,10-dionesemiquinone, $QNZ^{\bullet -}$ (Fig. 1). The semiquinones of benzo-1,4-quinone, $BQ^{\bullet -}$, and of phenanthraquinone, $PHQ^{\bullet -}$, were also studied for comparison.

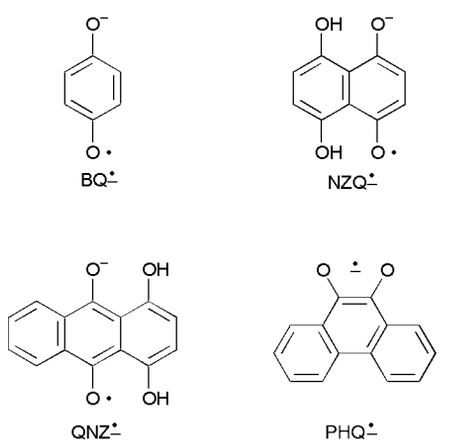

Fig. 1 Semiquinones studied in this work.

Experimental

Materials

The quinones NZQ (J. T. Baker), BQ (Pfaltz & Bauer), QNZ (Fluka), and PHQ (Aldrich Chemicals) were obtained from commercial sources. Quinones were purified by double sublimation and stored in a refrigerator. Spectrophotometric grade dimethyl sulfoxide, DMSO, was purchased from Aldrich. In order to improve the EPR spectra signal-to-noise ratios samples were prepared in a 1:1 v/v mixture of DMSO and 50 mmol dm^{-3} sodium cacodylate buffer at pH 7.4 where distilled, deionized water was used. As previously reported,[14] cacodylate was utilized instead of phosphate buffer to avoid precipitation of Mg^{2+}.

Semiquinone generation

Semiquinones were produced as previously described.[14,15] Since NZQ, QNZ and PHQ are slightly soluble in the buffer phase, semiquinones were first generated, under a nitrogen atmosphere, in absolute methanol by reacting from 10 to 20 mg of quinone with $NaBH_4$ in a convenient molar ratio such that semiquinone spectral intensity is maximized on transfer to aqueous buffer. The solution was then evaporated to dryness using a dry nitrogen flow. The sample was submitted to high vacuum for at least 30 min. A nitrogen-purged aqueous sodium cacodylate buffer solution, with or without $MgCl_2$, was then added to the dry semiquinone sample and the resulting solution equilibrated to pH 7.4 by addition of small aliquots of HCl or NaOH. This aqueous solution was diluted to 3.00 ml and centrifuged at 3500

DOI: 10.1039/b000540l

Table 1 Hyperfine coupling constants for the semiquinones under study here in nitrogen-saturated cacodylate buffer (pH 7.4) and the corresponding pK_a values

Semiquinone	a_H[a]/G	a_H[b]/G	pK_a
$BQ^{\bullet -}$	2.38 (4H′s)	2.35 (4H′s)	4.1[c]
$NZQ^{\bullet -}$	2.34 (4H′s), 0.59 (2 H′s)	2.356 (4H′s), 0.587 (2H′s)	2.7[d]
$QNZ^{\bullet -}$	2.25 (2H′s), 1.00 (2H′s), 0.61 (4H′s)	2.084 (2H′s), 0.905 (2H′s), 0.554 (2H′s), 0.520 (2H′s)	3.3[e]
$PHQ^{\bullet -}$	1.73 (2H′s), 1.60 (2H′s), 0.38 (4H′s)	1.73 (2H′s), 1.69 (2H′s), 0.41 (4H′s)	[f]
$PHQ–Mg^+$	1.75 (2H′s), 1.85 (2H′s), 0.41 (4H′s)		

[a] This work. [b] Ref. 18 (in alkaline aqueous solution). [c] Ref. 36. [d] Ref. 4. [e] Ref. 6. [f] pK_a values reported for *o*-semiquinones range from 3.6 to 5.2, ref. 37.

rpm for 5 min. The supernatant was then mixed with an equal volume of nitrogen-saturated DMSO to produce the final solution which was submitted to EPR analysis.

The semiquinone of BQ was generated by the comproportionation reaction between this quinone and its hydroquinone under nitrogen.

EPR measurements

First derivative EPR spectra were recorded on an X-band Bruker ER-200D EPR spectrometer coupled to a computer for data acquisition and analysis using the software developed by Morse.[16] Well-resolved semiquinone spectra were simulated and optimized (best-fitted to the experimental spectra) utilizing WINSIM[17] starting with hyperfine coupling constants available in the literature corresponding to aqueous or water-containing samples.[18] In the case where the free and the metal-complexed semiquinone spectra were observed simultaneously, EPR spectral intensity ratios were also obtained using WINSIM optimization.

Differences in the magnetic field positions of the semiquinones' first derivative EPR central peak between a sample without $MgCl_2$ and those corresponding to samples with increasing concentrations of this salt were measured using the dual-cavity technique,[19,20] where field/frequency lock was applied. For this purpose, the cavity was tuned with the presence of samples contained in septa-stoppered EPR quartz flat cells (60 × 10 × 0.25 mm). One of the samples in one resonator contained a semiquinone solution with no magnesium salt and the other a solution of the same semiquinone with a given concentration of $MgCl_2$. The spectral sweep width was decreased down to a value where only the semiquinone EPR spectral central peaks were isolated for both solutions and the magnetic field difference between these peaks was measured with two forward and two reverse scans which were averaged to a single field difference value. The difference in central peak position corresponding to two identical samples was subtracted from the measured values in order to correct for differences in magnetic field strengths between the resonators.

Best reproducibility was achieved if sample cells were not removed from the EPR dual cavity for a given batch of semiquinone solution. Thus, after measurements were made with a given sample, it was withdrawn from the sample cell using syringes, rinsed with water and replaced with another semiquinone sample with a different $MgCl_2$ concentration, after the sample had been rinsed once with this same solution.

Absorption UV–visible spectra

These were measured using a Beckman DU 7400, diode array UV–vis spectrophotometer.

Semiempirical theoretical calculations

Geometry optimizations using combined molecular mechanic (MM+) and open shell unrestricted SCF quantum chemical calculations (PM3/UHF, convergence limit 0.042 kJ mol^{-1}, RMS gradient 0.00042 kJ $Å^{-1}$ mol^{-1} and Polak–Ribiere conjugated gradient) were done with Hyperchem 5.1 (Hypercube Inc, Miami, FL). All molecular parameters were obtained from a single point calculation of the PM3 optimized structures. For the free semiquinones, the probability of having other local minima with lower energies near the considered minimum was decreased by using different starting structures. For the complexes, the magnesium cation was "added" to the previously optimized structure of the drug at different angles and distances and the complex energy minimum was reoptimized. The complex with the minimum energy was used for the calculation of the enthalpy of complex formation (reaction (1)) according

$$Q^{\bullet -} + Mg^{2+} \longrightarrow [Q–Mg]^{\bullet +} \quad (1)$$

to eqn. (2), where ΔH_1 is the enthalpy change of reaction (1)

$$\Delta H_1 = \Delta H_f(\text{complex}) - \Delta H_f(Q^{\bullet -}) - \Delta H_f(Mg^{2+}) \quad (2)$$

and ΔH_f are the corresponding enthalpies of formation. An enthalpy of formation of 483.5 kJ mol^{-1} was used for Mg^{2+}.[21] The values for the formation enthalpies of the complex and the semiquinone were obtained from the PM3 single point calculation of the corresponding species.

Results and discussion

Similar spectra to those reported in the literature were observed for the semiquinones under study in this work. Their EPR spectra were simulated and their corresponding hyperfine coupling constants were optimized as described in the Materials section, Table 1.

Upon addition of 0.6 mmol dm^{-3} $MgCl_2$ to a solution containing $PHQ^{\bullet -}$, a distortion in the symmetry of the corresponding EPR spectrum is observed (Fig. 2). Optimization of this spectrum assuming two different species produces a calculated spectrum which matches very well the experimental spectrum (correlation factor = 0.996) indicating that both the free and the metal-associated semiquinone spectra are observed simultaneously. The relative spectral intensities corresponding to these semiquinone species were obtained from this optimization, *i.e.* $[PHQ–Mg^+]/[PHQ^{\bullet -}] = 0.67 \pm 0.25$. From these intensities and the $MgCl_2$ concentration, and assuming that Mg^{2+} is not associated to Cl^- at this low salt concentration, a semiquinone–Mg^{2+} association constant was calculated to be $(1.1 \pm 0.5) \times 10^3$ dm^{-3} mol^{-1}.

Addition of up to 1.0 mol dm^{-3} of $MgCl_2$ to semiquinone solutions of NZQ, BQ and QNZ neither produces a new EPR spectrum nor changes the corresponding hyperfine coupling constants within experimental irreproducibility. However, a decrease in the corresponding semiquinone *g*-values was detected, as implied from an increase in the magnetic field value of the central spectral peak, upon salt concentration increase. A similar trend in *g*-value change has been reported previously and is due to semiquinone–metal ion association.[19,22] This observation indicates that the semiquinone–metal association/dissociation equilibrium is so fast on the EPR time scale that only a weighted average spectrum is detected for the associated and free species.[19] One could speculate that the observed spectra of these semiquinones, in the absence of $MgCl_2$, could be those

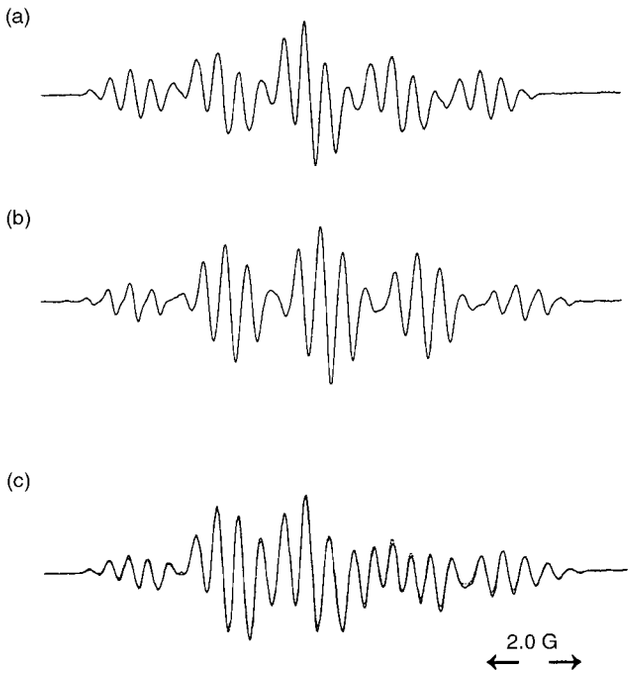

Fig. 2 EPR first derivative spectra of $PHQ^{\bullet -}$ corresponding to nitrogen-saturated aqueous solutions at pH 7.4 containing 50 mmol dm^{-3} sodium cacodylate buffer and (a) 0, (b) 100 and (c) 0.60 mmol dm^{-3} $MgCl_2$. Both the experimental (——) and calculated (····) spectra are shown superimposed in (c). The calculated spectrum was obtained using the hyperfine constants shown in Table 1 and a $[PHQ–Mg^+]/[PHQ^{\bullet -}]$ ratio of 0.67.

of the species complexed to trace transition metals which are always present in the glassware and buffer solutions.[23] However, addition of 0.1 mmol dm^{-3} desferrioxamine, which is a very strong chelator of transition metals,[24–26] did not produce a change in either the hyperfine constants or the *g*-values of the semiquinones.

From the corresponding changes in the central peak magnetic field, ΔH, the concentration ratio of the associated, β, to that of the free semiquinone, α, *i.e.* [β]/[α], can be determined. The semiquinone *g*-value of a salt-containing sample, g_{obs}, can be expressed in terms of the magnetic field position difference of the corresponding central peaks of this semiquinone and that of a semiquinone in a solution where no salt has been added, $\Delta H = H_{obs} - H_0$, eqn. (3), where the subscript "0"

$$g_{obs} = -\left(\frac{\Delta H}{H_{obs}}\right) g_0 + g_0 \qquad (3)$$

stands for the unassociated semiquinone and "obs" for the weighted average species.[19,27]

Since the observed *g*-value is a weighted average value, the ratio of the associated and unassociated species is given by eqn. (4),[19] where g' is the *g*-value of the associated complex, β.

$$\frac{[\beta]}{[\alpha]} = \frac{g_0 - g_{obs}}{g_{obs} - g'} \qquad (4)$$

Thus, the following relationship is easily demonstrated, eqn. (5).

$$\frac{[\beta]}{[\alpha]} = \frac{\Delta H_{obs}}{\Delta H' - \Delta H_{obs}} \qquad (5)$$

Therefore, the complex formation constant, K_1, could be obtained if the free Mg^{2+} concentration is known at each salt concentration value, eqn. (6). However, since large $MgCl_2$

$$K_1 = \frac{[\beta]}{[\alpha][Mg^{2+}]} \qquad (6)$$

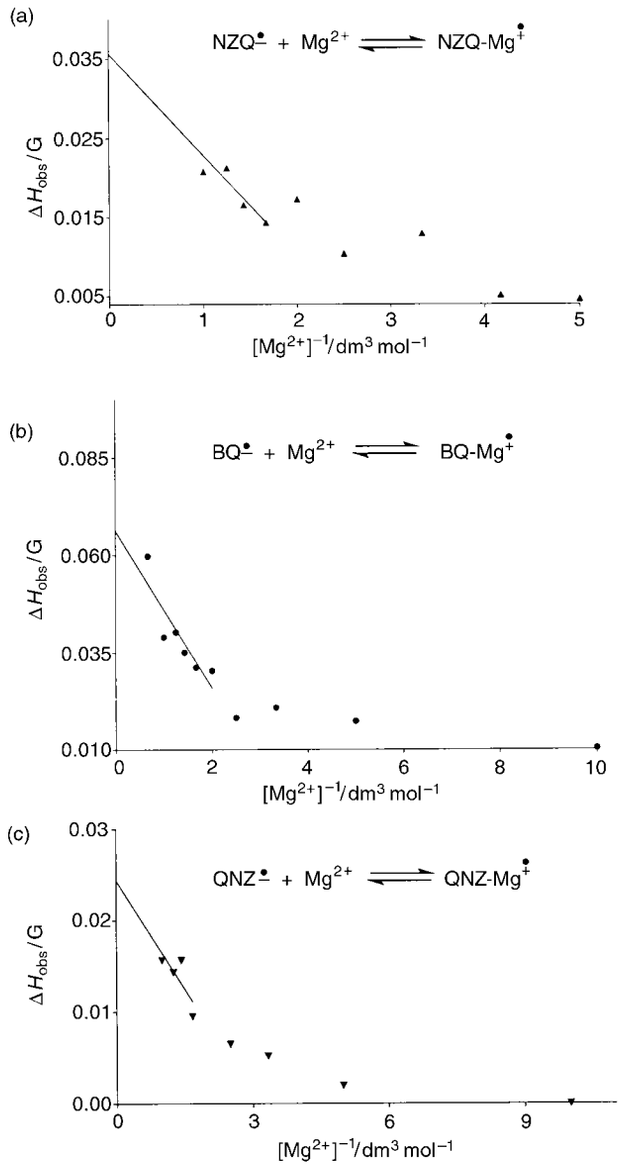

Fig. 3 Plots used in the extrapolation of $\Delta H'$ values for $NZQ^{\bullet -}$, $BQ^{\bullet -}$ and $QNZ^{\bullet -}$.

concentrations were used in this work in order to detect reproducible *g*-value shifts, it cannot be assumed that all of the magnesium cations are free in solution. In fact, Mg^{2+} association with Cl^- has been previously reported for aqueous solutions.[28,29] For a 0.33 M $MgCl_2$ aqueous solution, nearly 33% of the Mg^{2+} ions are associated with Cl^-.[22] However, the relative ability of each of the semiquinones under study here to interact with the magnesium cation can be obtained if the [β]/[α] ratio is determined at the same salt concentration or the rate of change of the [β]/[α] ratio with magnesium salt concentration is compared. In order to obtain the [β]/[α] ratios, $\Delta H'$ values were first determined by extrapolation of ΔH_{obs} to infinite salt concentration, *i.e.* to zero inverse salt concentration (Fig. 3). Since it has been previously shown that to obtain the most accurate values of the [β]/[α] ratios the saturation factor, *s*, should fall in the $0.2 \leq s \leq 0.8$ range,[30] eqn. (7), values of ΔH_{obs} were selected which correspond to s values near or within this range.

$$s = \frac{[\beta]}{[\alpha] + [\beta]} \qquad (7)$$

Values of [β]/[α] ratios, $\Delta H'$ and *s* are shown in Table 2. Plots of [β]/[α] against magnesium salt concentration roughly follow

Table 2 Representative data governing the semiquinone–Mg^{2+} complex formation equilibrium at 25 °C

$Q^{\bullet -}$	$[MgCl_2]$/M	$\Delta H'/10^{-2}$ G	[β]/[α]	s	$\frac{d([\beta]/[\alpha])^a}{d[MgCl_2]}$	$\Delta H_f{}^c/10^3$ kJ mol^{-1}
$NZQ^{\bullet -}$	0.4		0.47 ± 0.06	0.32		
	0.6		0.79 ± 0.09	0.44		
	1	3.56 ± 0.49	1.8 ± 0.2	0.64	2.2 ± 0.3	−1.38
$BQ^{\bullet -}$	0.4		0.39 ± 0.07	0.28		
	0.6		0.92 ± 0.10	0.48		−1.35
	1	6.50 ± 0.55	1.5 ± 0.3	0.6	1.7 ± 0.2	(−1.31)
$QNZ^{\bullet -}$	0.4		0.40 ± 0.05	0.29		
	0.6		0.73 ± 0.08	0.42		−1.43
	1	2.44 ± 0.26	2.2 ± 0.4	0.69	2.9 ± 0.4	(−1.39)
$PHQ^{\bullet -}$	6.0×10^{-4}	54[b]	0.67 ± 0.07		(1.1 ± 0.5)[d] × 10^3	−1.69

[a] Units: dm^3 mol^{-1}. [b] Obtained from optimization of spectrum as shown in Fig. 2. [c] Calculated enthalpies of complex formation. Values in parentheses correspond to complexes where the Mg^{2+} cation is located above the semiquinone molecular plane. [d] Estimated from the [β]/[α] value and the corresponding salt concentration.

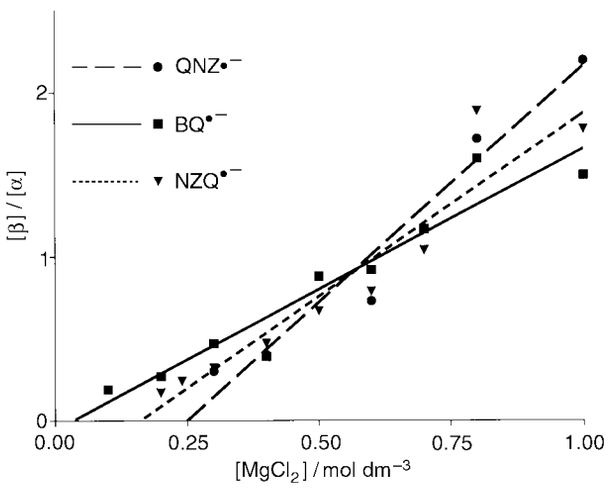

Fig. 4 Rates of change of the [β]/[α] ratios with magnesium salt concentration corresponding to $NZQ^{\bullet -}$, $BQ^{\bullet -}$ and $QNZ^{\bullet -}$.

straight lines (Fig. 4). The slopes of these lines are also shown in Table 2.

It can be observed from Table 2 that neither the [β]/[α] ratio values at a given salt concentration nor the slopes obtained from Fig. 4 are essentially different within experimental error for $NZQ^{\bullet -}$, $QNZ^{\bullet -}$ and $BQ^{\bullet -}$. Addition of $MgCl_2$, even in the mmol dm^{-3} range, to NZQ or QNZ solutions produces profound changes in the UV–visible spectra of these quinones, indicating a strong association of Mg^{2+} with these quinones (Fig. 5) which is consistent with the previously reported large formation constant of the QNZ complex with Mg^{2+}, *i.e.* $K_f = 10^4$ dm^3 mol^{-1}.[7] However, no variation in the BQ absorption spectrum was detected up to 400 mmol dm^{-3} $MgCl_2$. Thus, the hydroxysemiquinones, $NZQ^{\bullet -}$ and $QNZ^{\bullet -}$ are essentially as bad Mg^{2+} chelators as $BQ^{\bullet -}$ even though the parent hydroxyquinones have much larger affinities for this cation than BQ. In contrast, $PHQ^{\bullet -}$ binds Mg^{2+} quite efficiently, as observed from its high [β]/[α] ratio at a very low $MgCl_2$ concentration. This is also consistent with the fact that simultaneous observation of β and α occurs for $PHQ^{\bullet -}$ in contrast to the weighted average species detected for the other semiquinones. Tighter ion pairs such as that detected for $PHQ^{\bullet -}$ result in slow formation and dissociation of these within the EPR instrument time scale, thus permitting the simultaneous observation of both free and associated species.[19]

This difference in behavior between $NZQ^{\bullet -}$, $QNZ^{\bullet -}$ and $PHQ^{\bullet -}$ can be attributed to strong intramolecular hydrogen bonding between the hydroxy groups and the oxygen atoms of the hydroxysemiquinones. This strong hydrogen bonding interaction inhibits Mg^{2+} chelation, a fact that is also evidenced by

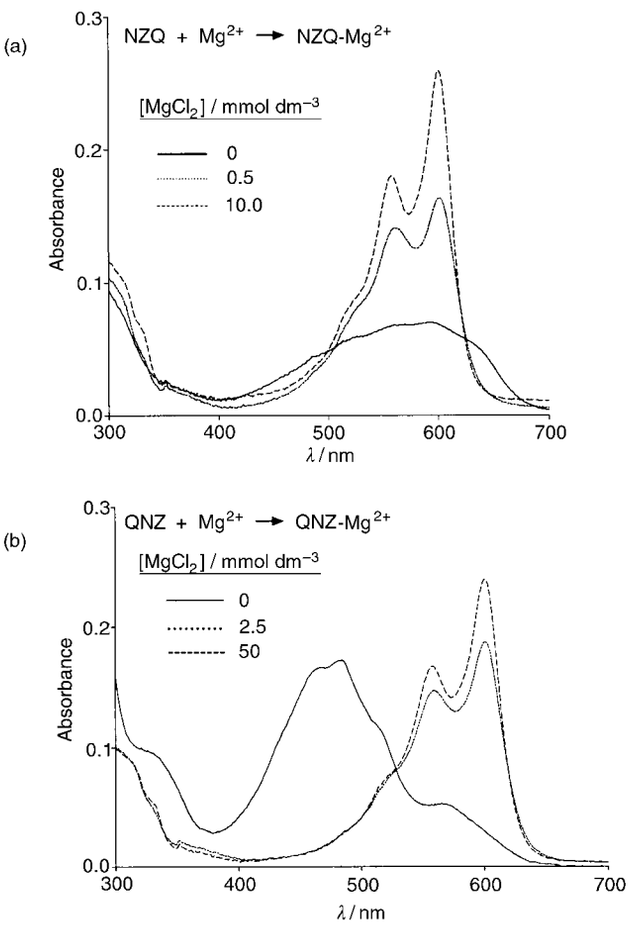

Fig. 5 Effect of $MgCl_2$ concentration on the (a) NZQ and (b) QNZ absorption spectra in a 1 : 1 v/v DMSO–H_2O mixture at pH 7.4 in the presence of 50 mmol dm^{-3} cacodylate buffer.

the invariance of the hyperfine splitting constants of these hydrogen-bonded protons with salt concentration increase. It has been reported previously that such hydrogen bond formation has profound effects on the corresponding semiquinone pK_a values[4] (pK_a values are lower than those corresponding to non-hydroxylated semiquinones) and on the semiquinone membrane/buffer partition constants.[14] Although the intramolecular hydrogen bonding existing in the parent quinones NZQ and QNZ shifts the visible absorption maxima of the corresponding non-hydroxylated quinones (naphthoquinone and anthraquinone) to longer wavelengths[31] and also affects the excited state stabilities and lifetimes of these quinones,[32,33] this is not as strong as needed to inhibit quinone–metal complex formation.

To account for the semiquinone structure effect on the complex equilibrium constant, combined quantum mechanical and semiempirical calculations (MM+/PM3) were performed on all species studied in this work. In general, the equilibrium constant of a reversible reaction is determined by the change in free energy (ΔG), which depends on the heat (ΔH) and entropy (ΔS) of the reaction. Since the entropy of a species depends in a complicated way on its modes of internal vibration, it is not possible to calculate it for big molecules. Therefore, the equilibrium constant of a reaction can only be predicted, relative to a given similar reaction and the ratio of the equilibrium constants for a pair of similar reactions (j and k) is determined by the corresponding reaction enthalpies, since they must have very similar reaction entropies ($\Delta S_j = \Delta S_k$), eqn. (8).[34]

$$\frac{K_j}{K_k} = e^{-\Delta\Delta G/RT} = e^{-(\Delta H_j - \Delta H_k)/RT} e^{(\Delta S_j - \Delta S_k)/R} \approx e^{-\Delta\Delta H/RT} \quad (8)$$

It is well known that ionic species have different degrees of solvation and therefore, reactions including these species have big entropy changes.[35] Nevertheless, solvation of an ion decreases both the entropy of the system and its heat content. Both changes tend to balance one another, so that the relative equilibrium constants of ionic reactions can still be estimated with the use of eqn. (8).[35]

The values obtained for the enthalpies of formation of the metal–semiquinone complexes are given in Table 2. Small differences were found between the enthalpies of complex formation if the magnesium cation was placed at a position of minimized energy above the semiquinone plane or coplanar with the semiquinone molecular frame. Although these enthalpies of formation corresponding to the complexes of $NZQ^{\bullet -}$, $BQ^{\bullet -}$ and $QNZ^{\bullet -}$ are within approximately 84 kJ mol^{-1}, this difference does not seem to predict differences in complex formation within the experimental error of our work. However, the enthalpy difference of complex formation between the most exergonic of the "weak" complexes group, *i.e.* $QNZ^{\bullet -}/Mg^{2+}$, and that corresponding to $PHQ^{\bullet -}Mg^{2+}$, *i.e.* $(1.69–1.43) \times 10^3 = 260$ kJ mol^{-1}, seems to be significant in predicting a large difference in complex formation ability.

Acknowledgements

The authors are grateful to NIGMS\MBRS for support of this work with grant no. SO6-GM08216.

References

1 T. Friedrich, A. Abelmann, B. Brors, V. Guenebaut, L. Kintscher, K. Leonard, T. Rasmussen, D. Scheide, A. Schlitt, U. Schulte and H. Weiss, *Biochim. Biophys. Acta*, 1998, **1365**, 215.
2 T. Friedrich, K. Steinmuller and H. Weiss, *FEBS Lett.*, 1995, **367**, 107.
3 P. Wardman, M. F. Dennis, S. A. Everett, K. B. Patel, M. R. Stratford and M. Tracy, *Biochem. Soc. Symp.*, 1995, **61**, 171.
4 E. J. Land, T. Mukherjee and J. Swallow, *J. Chem. Soc., Faraday Trans. 1*, 1983, **79**, 391.
5 S. I. Bailey and I. M. Ritchie, *Electrochim. Acta*, 1985, **30**, 3.
6 T. Mukherjee, A. J. Swallow, P. M. Guyan and J. M. Bruce, *J. Chem. Soc., Faraday Trans.*, 1990, **86**, 1483.
7 R. Kiraly and R. B. Martin, *Inorg. Chim. Acta*, 1982, **67**, 13.
8 P. M. May, G. K. Williams and V. R. Williams, *Eur. J. Cancer*, 1980, **16**, 1275.
9 D. A. Gewirtz, *Biochem. Pharmacol.*, 1999, **57**, 727.
10 C. Hershko, A. Pinson and G. Link, *Acta Haematol.*, 1996, **95**, 87.
11 T. Masahiko and I. Masamoto, *Nippon Kagaku Kaishi*, 1988, **4**, 701. (Japanese, from Chemical Abstracts Service # 109:84996.)
12 B. A. Svingen and G. Powis, *Arch. Biochem. Biophys.*, 1981, **209**, 119.
13 E. J. Land, T. Mukherjee, A. J. Swallow and J. M. Bruce, *Arch. Biochem. Biophys.*, 1983, **225**, 116.
14 A. E. Alegria, S. Rivera, M. Hernandez, R. Ufret and M. Morales, *J. Chem. Soc., Faraday Trans.*, 1993, **89**, 3773.
15 A. E. Alegria, M. Lopez and N. Guevara, *J. Chem. Soc., Faraday Trans.*, 1996, **92**, 4965.
16 P. D. Morse II, *Methods Enzymol.*, 1986, **127**, 239.
17 D. R. Duling, *J. Magn. Reson., Ser. B*, 1994, **104**, 105.
18 J. A. Pedersen, *Handbook of EPR Spectra from Quinones and Quinols*, CRC Press, Boca Raton, 1985.
19 G. R. Stevenson, A. McB. Block and A. E. Alegria, *J. Am. Chem. Soc.*, 1975, **97**, 4859.
20 M. T. Jones, R. Ahmed, R. Kastrup and V. Rapini, *J. Phys. Chem.*, 1979, **83**, 1327.
21 R. A. Alberty and R. J. Silbey, *Physical Chemistry*, Second edition, Wiley, New York, 1997, p. 875.
22 A. E. Alegría and B. Velázquez, *J. Solution Chem.*, 1992, **21**, 1241.
23 G. R. Buettner, *Methods Enzymol.*, 1990, **186**, 125.
24 R. Munday, *Free Radical Biol. Med.*, 1997, **22**, 689.
25 Y. Li and M. A. Trush, *Arch. Biochem. Biophys.*, 1993, **300**, 346.
26 S. G. Sullivan and A. Stern, *Biochem. Pharmacol.*, 1981, **30**, 2279.
27 J. E. Wertz and J. R. Bolton, *Electron Spin Resonance: Elementary Theory and Applications*, McGraw-Hill, New York, 1972, pp. 464–465.
28 A. De Robertis, C. Rigano, S. Sammartano and O. Zerbitani, *Thermochim. Acta*, 1987, **115**, 241.
29 H. S. Harned and B. B. Owen, *The Physical Chemistry of Electrolytic Solutions*, 3rd edition, Rheinhold, New York, 1958.
30 D. A. Deranleau, *J. Am. Chem. Soc.*, 1969, **91**, 4044.
31 J. M. Malcolm, in *The Chemistry of Quinonoid Compounds*, ed. S. Patai, Wiley, London, 1974, Part 1, Chap. 9.
32 E. J. Land, T. Mukherjee and J. Swallow, *J. Chem. Soc., Faraday Trans. 1*, 1983, **79**, 391.
33 D. K. Palit, P. Haridas, T. Mukherjee and J. P. Mittal, *J. Chem. Soc., Faraday Trans.*, 1990, **86**, 3861.
34 J. A. Pople and D. L. Beveridge, *Approximate Molecular Orbital Theory*, McGraw-Hill, New York, 1970, pp. 85–88.
35 M. J. S. Dewar and R. C. Dougherty, *The PMO Theory of Organic Chemistry*, Plenum Press, New York, 1975, pp. 131–138.
36 Y. A. Ilan, G. Czapski and D. Meisel, *Biochim. Biophys. Acta*, 1976, **430**, 209.
37 B. Kalyanaraman, *Methods Enzymol.*, 1990, **186**, 333.